Research Article

Christopher Essex and Bjarne Andresen

Maxwellian velocity distributions in slow time

Abstract: We extend Maxwellian velocity distributions to long observational timescales in much the same way that short timescale statistical mechanics distributions are averaged to yield normal laboratory timescale thermodynamic distributions. This long timescale view has several novel effects: Fluctuating overall velocities (i.e. "wind") thermalizes into an additional component of temperature, while returning a Maxwellian velocity distribution. However, fluctuating temperature results in a new distribution with a Gaussian core but heavy polynomial tails. The power of the polynomial tail is either -3 or -2 depending on whether the precision of the temperature is allowed to extend to $\pm$ infinity or is required to remain strictly positive. The distribution is also interesting in the way it remains almost exactly Gaussian up to a certain velocity after which it quickly breaks off to become polynomial. The distributions are carefully analyzed mathematically, and physical consequences are drawn.

Keywords: Slow time, long time, Maxwellian

Christopher Essex: Department of Applied Mathematics, The University of Western Ontario, London, Ontario N6A 5B7, Canada, e-mail: essex@uwo.ca
Bjarne Andresen: Niels Bohr Institute, University of Copenhagen, Universitetsparken 5, DK-2100 Copenhagen Ø, Denmark, e-mail: andresen@nbi.ku.dk

Communicated by: Paolo Sibani and Karl Heinz Hoffmann

1 Introduction

The kinetic domain brings to mind Brownian movement, individual molecules colliding, and dust particles jiggling. This microscopic chaos becomes invisible in the limit of the larger scales of space, time, and particle number that define the laboratory domain. Historically, linking the microscales to the laboratory scales is the subject of statistical mechanics and kinetic theory. The laboratory scales function as an ideal, guiding us among the various possible averaging processes that could take a discrete domain over to apparent continua, allowing the microscopic chaos to be subsumed within thermodynamic equilibrium. But thermodynamic equilibrium is also a limiting case that is realized rarely even as an approximation. In the continua of the laboratory regime we do not typically achieve thermodynamic equilibrium at all. But if we imagine traveling with the various dynamics that may exist in continua, we have a useful and pervasive alternative, local thermodynamic equilibrium (LTE). In the mechanical rest frame of a moving fluid we imagine that we may measure temperature and pressure locally as if the fluid were in equilibrium even if globally it is not. This is the normal framework in which pressure, temperature, and other intensive quantities were first encountered historically, and it is the primary way we experience them in our lives – through meteorological and biological temperatures, for example.

But while this local equilibrium is essential for many fields, employing classical treatments of physics and chemistry, it is inherently limited. For example photons are typically not near equilibrium locally even if the interacting particles having mass may be. These words would be invisible otherwise. The classical Maxwellian distribution for particle velocities will hold locally, but not without limitations if temperature can be meaningfully represented as a continuous function of position in configuration space where the discrete particles with that distribution are also located. Atoms or molecules from spatially nearby local equilibria must therefore interact, meaning that the local equilibria are inherently transient if not externally controlled. In order for them not to relax to a common equilibrium, processes must drive these local states to remain apart, thus

never quite relaxing to a formal Maxwellian. The relaxation time to full equilibrium must be longer than the timescales of the processes that form the laboratory scale gradients.

While we are not aware of any previous attempts at identifying slow time behavior as a separate dynamics, we did recently look into a more precise definition of the viability of local thermodynamic equilibrium [1] mentioned above, i.e. when is it realistic to talk about LTE values of say temperature and pressure. The requirement is that time should be sufficiently short that essential equilibration is achieved within the (small) local volume but not within the entire system. In the space of all extensive thermodynamic variables such local equilibria will appear as a swarm of points. Only when true global equilibrium is achieved will they merge into a single point.

Clearly, with a large but finite number of molecules there is a place in the infinite tails of the distributions that is relatively unpopulated. The particles in the sparsely populated tails will also be the particles moving the quickest, and so would have the shortest interaction times as they move most rapidly to local equilibria neighboring in configuration space. Thus we expect to find the greatest departure from a limiting Maxwellian in the tails of the local equilibrium distributions. But if the spatial and temporal resolutions are lower than that over which local equilibria vary, then the observed probability density will be a composition of many local equilibria in space and time and not just one.

A number of fields encounter such distributions of distributions, or distributions subordinated other distributions. For example, many spin glasses and random field systems have time evolutions which are statistically subordinated sudden jumps in energy (quakes or avalanches) [2, 3]. In cosmology dark matter distributions are frequently convolved in such a way [4] that the new distribution may be described by a non-extensive Tsallis distribution [5]. Porous media are often described by models which include combinations of thermodynamic distributions and geometric restrictions [6] or diffusion on a fractal support [7]. Studies on spiking responses of motor cortical neurons display a firing rate described best by a convolution of expected single neuron response with a distribution of other extraneous inputs [8]. Many of these convoluted distributions have heavy polynomial tails. Generically, something like this is always at play when we study mutual information. However, none of the situations mentioned above as well as many other situations are relevant to the long time behavior we are investigating here.

1.1 Slow time

Any experiment or any observer is limited to a certain time window. We cannot distinguish between physical events that are too close together in time. We cannot even recognize the order of the events, raising questions about causality. Similarly, connected events too far apart in time are also not recognized. But that is because they seem unconnected. Changes are too slow to observe directly. Our only hope to comprehend such things is indirectly through inference from evidence left by the changes. Continental drift is a classical example. We do not see it directly but the rocks tell us what happened outside of our lifetimes, outside of our window of perception. Events that are too close together to perceive we say are beyond our *fast time* limit, while events that are too far apart to perceive we say are beyond our *slow time* limit. We refer to the slow time regime as being beyond the slow time limit. Figure 1 illustrates this. Sally Shortwave was coined to represent an idealized observer on nanoscales. Larry Longwave represents observers on scales of years, lifetimes, or eons. Our everyday lives are somewhere in between. Great effort has been expended in comprehending what an observer encounters in the regime of Sally Shortwave. In this paper we attempt to get a glimpse into what an observer in Larry Longwave's regime would perceive.

With instruments that are too coarse and slow to capture local (near) equilibria, the observer would not be able to perceive the laboratory scales that we know, but would observe a folding of many local states within one. From the point of view of distributions, the observer would encounter a composite distribution instead. That observer would perceive the laboratory scales the way we think of Sally Shortwave's regime. That is, it would seem remote, abstract, and invisible, only accessible through inference and clever experiments. The scalar fields of local thermodynamic variables and their temporal variations, which are central to our expe-

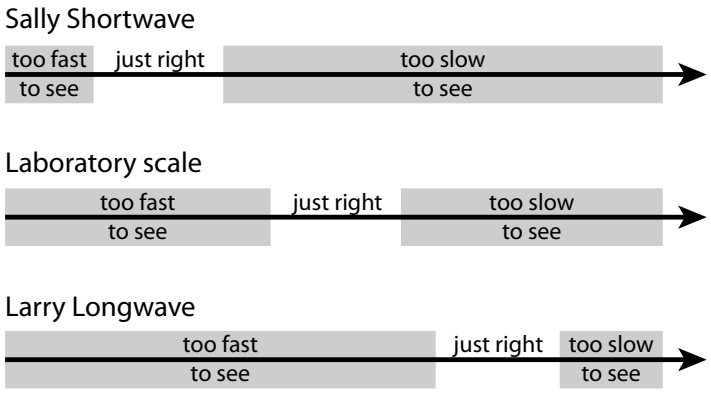

Figure 1. Any experiment or any observer is limited to a certain time window within which it is able to achieve time resolution and thus establish 'before' and 'after' and causality. At shorter times we cannot resolve that, at longer times we do not observe any change. Sally Shortwave lives in the nanoscales world, Larry Longwave in a world of years or eons. Our everyday lives are somewhere in between.

rience, would be unknown to that observer. They would be like jiggling molecules are to us. But what would the observer see that would be foreign to our experience?

Would the observer in Larry's regime see our laboratory scale as we do the nanoscale? What would his regime be like? Would it be able to stand on its own, as does the laboratory regime, or would it be necessary to constantly consult the underlying scales to faithfully represent it? That is, could it be closed? Just as the mechanics of nanoscales differs from our experience being jiggly, sticky and non-inertial, should we expect a different mechanics for his regime? Would there be a kind of thermodynamics distinct to this regime?

1.2 Objectives

This paper attempts to discover what the Maxwellian distribution becomes beyond the slow time limit, i.e. the *slow time Maxwellian*. This is needed before pursuing slow time analogues to fluid mechanics or local thermodynamic equilibrium. Some preliminary conceptual ideas have been published in [9, 10]. While we take an approach similar to classical statistical mechanics, ours is more speculative because we are not aiming to connect two known regimes. The slow time regime is not currently known.

Space scales accompany timescales. If a collection of particles have a characteristic speed, their ability to interact with surrounding particles is limited spatially when given a particular timescale. Groups of particles beyond this characteristic distance are independent, while on longer timescales they are not. Thus to consider the slow time behavior one must consider a box with space coordinates and time. The box only represents the sampling space, allowing particles to pass freely.

To ensure one is not just constructing an ensemble of particles that will recover the classical Maxwellian behavior for the laboratory regime, we imagine that the box is composed of small cells each having its own local statistics defined by a local Maxwellian with a temperature T and a rest frame velocity u. This is the fluid mechanical rest frame (mean). Other rest frames may be defined for other flow variables of the system. Their rest frame velocities frequently differ from u. We then proceed with distributions in u and T to capture the distribution of the entire space-time box. This picture treats local velocity u and temperature T as representing fluctuations in local particle states within cells. Since the slow time regime treats the box as the limit of resolution, the distribution of the box becomes the observed particle distribution, which is the composition of the individual Maxwellians within it.

We first consider the effect of a fluctuating mean velocity u about 0 for fixed T. As u is not only the rest frame velocity, but becomes the wind of fluid mechanics, there is a trade off between wind and temperature on long timescales. The new temperature θ appears as it normally does in equilibrium, but for a slow time equilibrium. Thus for fixed T a slow time ideal gas has a revised temperature θ which emerges in velocity

moments generating all of the standard expressions in place of T. Wind becomes thermalized not by process but by resolution.

However, things are not so neat when temperatures fluctuate, because temperature also appears in the normalization of the distribution. The resulting distribution is not Gaussian any longer. It is a distinctive hybrid with a Gaussian core and heavy tails. The issue of heavy tails is explored, and the results of different assumptions are compared.

Specific values for constants are important to develop a sense of the relative contributions of terms. The values used are far from unique, but for the purposes of this paper values representing air at room temperature are set in Appendix A and described as standard values throughout.

2 Thermalization of wind

Preliminary to other fluctuations, we consider the effect of fluctuations in rest velocity, u, or wind. Without loss of generality we proceed in terms of fluctuations in one space dimension. Then the molecular velocity profile is

$$p(v;u,T) = \left(\frac{m}{2kT}\right)^{1/2} \frac{1}{\sqrt{\pi}} \exp\left(-\frac{m}{2kT}(v-u)^2\right). \tag{1}$$

Imagine that within a space-time box large enough winds experience reversals and ranges of magnitudes so that we may plausibly assume a normally distributed rest velocity u about $u = 0$ with σ_u being its standard deviation, used for a Maxwellian probability distribution function (PDF) with temperature T. It is conceivable that no circumstance occurs where the central limit theorem fully holds. However assuming it does, this convolution of the v and u distributions is itself a Gaussian,

$$p(v;\theta) = \left(\frac{m}{2k\theta}\right)^{1/2} \frac{1}{\sqrt{\pi}} \exp\left(-\frac{m}{2k\theta}v^2\right), \tag{2}$$

but with a revised effective temperature

$$\theta = \frac{\sigma_u^2 m}{k} + T \tag{3}$$

that contains the wind u. Suppose $\sigma_u \sim 5$ m/s, then $\sigma_u^2 m/k \sim 0.1$ K (see Appendix A). This change of temperature of 0.1 K is negligible under normal conditions.

Generalizations of temperature are a standard fare of extended irreversible thermodynamics (e.g., [11, 12]). There are also temperature analogues that become temperature under limiting conditions (e.g., [13]). But the emerging temperature here, θ, is like neither of these: It is an emergent feature of a well-defined underlying mechanism. The presence of small underlying fluctuations may bring to mind concepts like contact temperature (e.g., [14]), where small deviations in flows affect what an instrument actually reads. But this is also a different problem. The present θ is in all respects a legitimate temperature and not just a generalization. As long as u is fluctuating in a Gaussian manner, all of the ideal gas relationships re-emerge, but in the temperature θ instead of T. For example energy E along one axis is simply, $E = Nk\theta/2$, just as it is in T for the laboratory regime. Coarsening the time scale for fluctuations in u amounts to thermalizing the wind.

3 Fluctuations in temperature

It will prove to be mathematically and conceptually convenient to work with the Gaussian precision (defined below) instead of the standard deviation in what follows. For such distributions of distributions, fluctuations in standard deviation are proportional to fluctuations in the square root of temperature. A fluctuation in precision would be in terms of $\sqrt{\beta}$ ($\beta = 1/(kT)$) instead. A larger precision means a tighter distribution. This is well precedented. Similar structures are in play for thermodynamic intensive variables, like pressure and chemical potential. P, μ, and β are all conjugate to V, N, and E, respectively, while temperature is the odd variable residing in the denominator in that representation.

There is no particular reason *a priori* to presume that fluctuations in T, or some function of T, are normally distributed. This is speculation, but in any event all such assumptions cannot be strictly true simultaneously. The aim is only to find a plausible slow time scenario, although we will find the outcome appears to be quite similar with different assumptions. The differences will be explored in plots from direct computations below. Meanwhile we will not be working with T but $\theta = 1/(k\beta_\theta)$, where wind, u, has been thermalized. Moreover, we will still refer to fluctuations in the precision as "temperature fluctuations."

The Gaussian precision, ψ, is defined by the following,

$$\left(\frac{m}{2k\theta}\right)^{1/2}\frac{1}{\sqrt{\pi}}\,\exp\left(-\frac{m}{2k\theta}v^2\right) = \frac{\psi}{\sqrt{\pi}}\,\exp(-\psi^2 v^2), \tag{4}$$

where ψ is given by $\psi = 1/(\sqrt{2}\sigma_\theta) = \sqrt{m/(2k\theta)} = \sqrt{m\beta_\theta/2}$ and has units of 1/velocity for the Maxwellian.

Let us now suppose that this precision itself is not constant but is normally distributed in a variable ξ about some reference value ψ_0 such that $\psi = \psi_0 + \xi$. Then

$$\frac{\psi}{\sqrt{\pi}}\,\exp(-\psi^2 v^2) = \frac{\psi_0+\xi}{\sqrt{\pi}}\,\exp(-(\psi_0+\xi)^2 v^2) \equiv p_{v\xi}. \tag{5}$$

Because $\psi = \sqrt{m/2k\theta} > 0$ for finite θ then $\xi \in (-\psi_0, \infty)$, so that the normal distribution ought to be truncated. However, in typical statistical applications infinite domains are commonly used instead of semi-infinite ones. For example, the convention of spectroscopy is to integrate over spectral lines for frequencies, $\nu \in (-\infty, \infty)$, even though negative frequency makes little physical sense. If we anticipate, as in spectroscopy, that little is lost because the inadmissible values contribute little to relevant integrals, this can be a viable approach, which can be checked after the fact.

Taking this position we allow $\xi \in (-\infty, \infty)$ instead. The corresponding PDF in ξ is

$$\hat{p}_\xi = \frac{w}{\sqrt{\pi}}\,\exp(-w^2\xi^2), \tag{6}$$

where w is the Gaussian precision for this ξ distribution with units of velocity. The hat (caret) indicates the infinite domain extension. We will see that the resulting structure is such that w appears naturally in the expressions as a velocity aiding interpretation of molecular velocity v regimes:

$$\hat{p}(v; w, \psi_0) = \int_{-\infty}^{\infty} p_{v\xi}\hat{p}_\xi d\xi = \frac{w^3\psi_0}{\sqrt{\pi}(v^2+w^2)^{3/2}}\,\exp\left(-\frac{w^2\psi_0^2 v^2}{v^2+w^2}\right). \tag{7}$$

Two distinctive features emerge: This PDF has polynomial (heavy) tails and a Gaussian core. The shift between these is controlled by the remarkable argument of the exponential, $-w^2\psi_0^2 v^2/(v^2+w^2)$. When $v \ll w$, it becomes the classical Gaussian argument $-\psi_0^2 v^2$ since the denominator in the pre-factor, $(v^2+w^2)^{3/2}$, behaves like a constant. When $v \gg w$, the argument of the exponential approaches a constant leaving an asymptotic behavior of $\sim v^{-3}$.

This is quite different from the result of letting the velocity u fluctuate, where the result was another Gaussian PDF, but with a revised temperature, θ. The u fluctuations were naturally incorporated into the microscopic ones. This does not happen with the fluctuations in ξ since temperature or precision also appears in the normalization factor multiplying the exponential.

For the truncated distribution $\hat{p}_\xi$ of ξ, equation (6) gets replaced by

$$p_\xi = \frac{2}{1+\operatorname{erf}(w\psi_0)}\frac{w}{\sqrt{\pi}}\,\exp(-w^2\xi^2). \tag{8}$$

If $\psi_0 \to \infty$ the error function goes to 1, causing the expression to reduce to the Gaussian on the infinite domain with the function always normalized to 1. For the standard values defined in Appendix A, one has $2/(1+\operatorname{erf}(w\psi_0)) \approx 2 - 10^{-7}$, which makes (6) close to (8) despite different normalizations.

Then the new velocity distribution is given by the density function

$$p(v;w,\psi_0) = \int_{-\psi_0}^{\infty} p_{v\xi}\, p_\xi\, d\xi$$

$$= \frac{1+\operatorname{erf}\left(\frac{w^2\psi_0}{(v^2+w^2)^{1/2}}\right)}{1+\operatorname{erf}(w\psi_0)} \frac{w^3\psi_0}{\sqrt{\pi}(v^2+w^2)^{3/2}} \exp\left(-\frac{w^2\psi_0^2 v^2}{v^2+w^2}\right) + \frac{1}{1+\operatorname{erf}(w\psi_0)} \frac{w}{\pi(v^2+w^2)} \exp(-w^2\psi_0^2). \quad (9)$$

The second term arises because of the truncation, which no longer permits an odd term in the integrand from canceling out under integration. It is thus responsible for a quadratic heavy tail, which will dominate the cubic one in the first term for large v. The mathematical nature and physical meaning of this difference will be discussed in the following. But it bears noting that this term's existence is entirely a consequence of asymmetric truncation, which can be as physically questionable as any of the other assumptions.

3.1 Common limits

The large w limit (infinite ξ precision, i.e. no ξ fluctuations) removes all temperature fluctuations:

$$\lim_{w\to\infty} p(v;w,\psi_0) = p(v;\infty,\psi_0) = \hat{p}(v;\infty,\psi_0) = \frac{1}{\sqrt{\pi}}\psi_0 \exp(-\psi_0^2 v^2) \equiv p_{\psi_0}. \quad (10)$$

For $v \ll w$ for given finite w, the second term of (9) is negligible and then

$$p(v;w,\psi_0) \approx \frac{1}{\sqrt{\pi}}\psi_0 \exp(-\psi_0^2 v^2) \approx \hat{p}(v;w,\psi_0), \quad (11)$$

i.e. the same result as for large w. Thus near the center of the PDF the function behaves like a Maxwellian with temperature θ while far from the core the simple notion of temperature is not sustainable. This Maxwellian is invalid for $|v| > |w|$, thus θ has no usable role in the sense of thermodynamics in that moments of the integral will not produce the traditional simple functions in terms of θ. For example the second moment diverges. What that means will be discussed below.

3.2 Compound probability distributions

In order to illustrate the effect of temperature variations we have calculated a number of velocity distributions with different standard deviations in Figure 2 (the thin red curves). Averaging such velocity distributions over three different temperature variations – a Gaussian distribution of the standard deviations (fat red), a boxcar distribution of the standard deviations (fat blue), and a Gaussian distribution in precision of the precisions (fat green) – results in velocity distributions distinctly wider than a Gaussian. The distributions of standard deviations σ_v and precisions ξ_v used for these compound probability distributions are depicted in Figure 3. The slight difference between the standard deviation (red) and precision (cyan) curves indicates the small difference in using one or the other averaging method.

4 The scaling function Λ

Define a function $\Lambda(v;w,\psi_0)$ such that it transforms the infinite domain probability distribution into the truncated one,

$$p(v;w,\psi_0) = \hat{p}(v;w,\psi_0)\Lambda(v;w,\psi_0). \quad (12)$$

Λ provides an effective framework, not only to understand the relationship between p and $\hat{p}$, but to understand the nature of the transition from Gaussian to heavy tails for both functions.

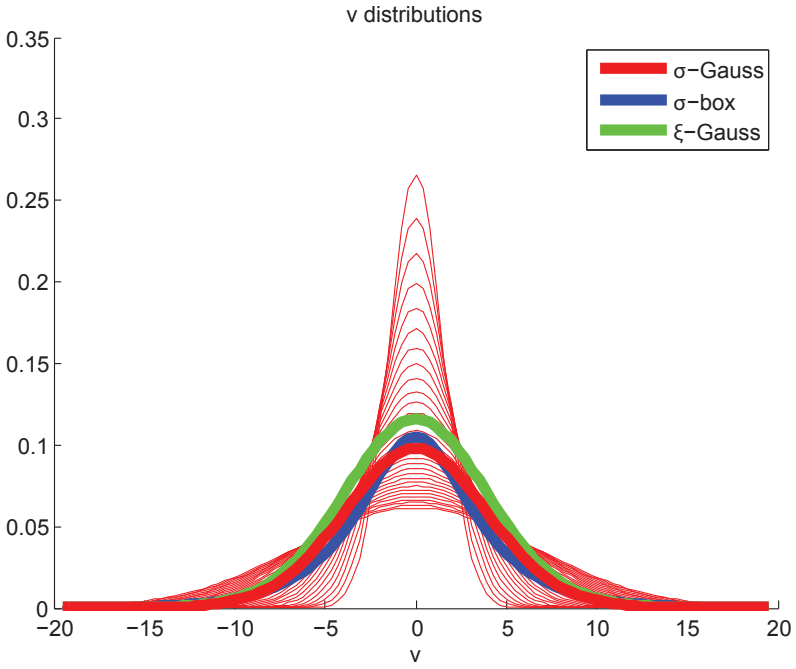

Figure 2. Velocity distributions for different variations. The thin red curves are Gaussian distributions for standard deviations $\sigma_v \in [1.5, 6.5]$ m/s. The fat curves are velocity distributions averaged over a range of deviations. The red curve is averaged over a Gaussian distribution of σ_v itself having a standard deviation of 0.5 m/s around 4.0 m/s. The blue curve is averaged over a boxcar distribution of σ_v in the range $[3.5, 4.5]$ m/s. And finally the green curve is the velocity distribution with a variable precision corresponding to the red standard deviation curve; they are pinned at ± 1 standard deviation of both. Clearly the type of averaging makes only a minor difference for these purposes.

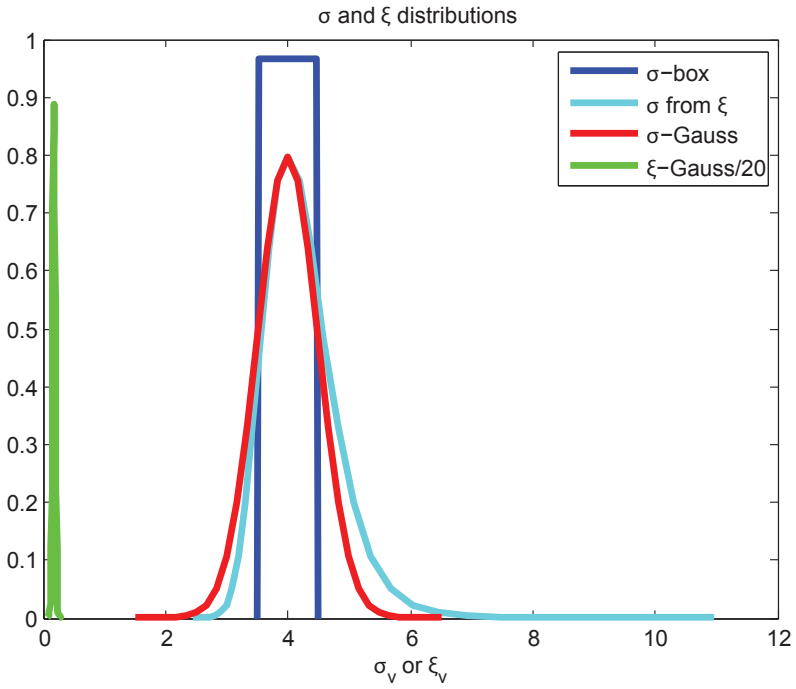

Figure 3. Distributions of standard deviations σ_v and precisions ξ_v used for the averages of Figure 2. Blue is the boxcar distribution of σ_v. Red is the Gaussian distribution of σ_v. And green is the precision distribution of the precision ξ (scaled down by a factor of 20 to fit on the same plot). Finally, the cyan curve is a conversion of the green precision distribution into equivalent standard deviations. The slight difference between the red and cyan curves indicates the small difference in using one or the other averaging method.

From (9) and (7) it follows that

$$\Lambda(v;w,\psi_0) = \frac{1}{1+\operatorname{erf}(w\psi_0)}\left[1+\operatorname{erf}\Big(\frac{w^2\psi_0}{(v^2+w^2)^{1/2}}\Big)+\frac{(v^2+w^2)^{1/2}}{\psi_0\sqrt{\pi}w^2}\,\exp\Big(-\frac{w^4\psi_0^2}{v^2+w^2}\Big)\right] \tag{13}$$

and

$$\lim_{w\to\infty}\Lambda(v;w,\psi_0) = \Lambda(v;\infty,\psi_0) = 1. \tag{14}$$

Thus $p(v;\infty,\psi_0) = \hat{p}(v;\infty,\psi_0)$ returning both distributions to the no temperature fluctuation case.

Λ is an extraordinary function as can be seen from its graph (Figure 4). It takes on the value 1 with remarkable precision for a wide interval in v out to values in excess of 10^7 m/s for our standard values, which approaches 10% of the speed of light. Beyond that, asymptotically linear growth ensues because the two different heavy tails diverge from each other as $\hat{p}$ decreases more rapidly than p.

The most extraordinary features of Λ are in the details. To understand this function take the derivative

$$\frac{d\Lambda}{dv} = \frac{1}{(1+\operatorname{erf}(w\psi_0))\sqrt{\pi}\psi_0 w^2}\,\frac{v}{(v^2+w^2)^{1/2}}\,\exp\Big(-\frac{w^4\psi_0^2}{v^2+w^2}\Big). \tag{15}$$

As Λ is symmetric, we need to look only at positive v in the following treatment of the derivative. For $v \ll w$,

$$\frac{d\Lambda}{dv} \sim \frac{v}{(1+\operatorname{erf}(w\psi_0))\sqrt{\pi}\psi_0 w^3}\,\exp(-w^2\psi_0^2) \approx 10^{-13}\times 10^{-2.7\times10^4}v, \tag{16}$$

using the standard values in Appendix A. Here, 10^{-13} is the contribution of the factors other than the exponential, which are clearly of no significance. Even though the derivative is increasing with v, the coefficient is so extraordinarily small that with increasing v it will be indistinguishable from zero to computer accuracy well beyond $v = w$. But above $v = w$, the exponential factor in (15) ceases to behave like a constant. The denominator of the exponential's argument begins to grow significantly and the exponential begins to grow toward 1 rapidly. We see that

$$\lim_{v\to\infty}\frac{d\Lambda}{dv} = \frac{1}{(1+\operatorname{erf}(w\psi_0))\sqrt{\pi}\psi_0 w^2}, \tag{17}$$

i.e. the slope approaches a constant.

Because the first derivative is so small compared to 1, the second derivative

$$\frac{d^2\Lambda}{dv^2} = \frac{v^2(1+2w^2\phi_0^2)+w^2}{(1+\operatorname{erf}(w\psi_0))\sqrt{\pi}\psi_0}\,\frac{1}{(v^2+w^2)^{5/2}}\,\exp\Big(-\frac{w^4\psi_0^2}{v^2+w^2}\Big) \tag{18}$$

is the curvature. Figure 5 shows that it rises from essentially zero to a maximum somewhat above w, then drops off to zero again. The maximum is the smallest radius of curvature in the natural metric, which would not necessarily be apparent on a plot of arbitrary units. This behavior suggests a bend between nearly straight lines, which is what we observe; see Figure 4.

Before the turn, both p and $\hat{p}$ behave like the Gaussian they have in common, p_{ψ_0} (see limits (10) and (11)), which is why Λ is steadily close to 1. After the turn, $|v| \gg |w|$, they differ in how heavy their respective heavy tails are. The infinite domain case, $\hat{p}$, is cubic and the truncated domain case, p, is quadratic. This demonstrates that the heavy tail behavior originates with fluctuating temperature as the presence of heavy tails is controlled by the precision w. The larger the value of w the further out in v the p_ψ-like behavior extends.

5 The scaling function Φ

Λ compared two hybrid heavy-tail/Gaussian distributions. We must also compare the hybrid densities with fluctuating precision to the pure Gaussian forms with fixed precision to complete the investigation. Define Φ such that $\hat{p}(v;w,\psi_0) = p_{\psi_0}\Phi$, then

$$\Phi = \frac{w^3}{(v^2+w^2)^{3/2}}\,\exp\Big(\frac{\psi_0^2v^4}{v^2+w^2}\Big). \tag{19}$$

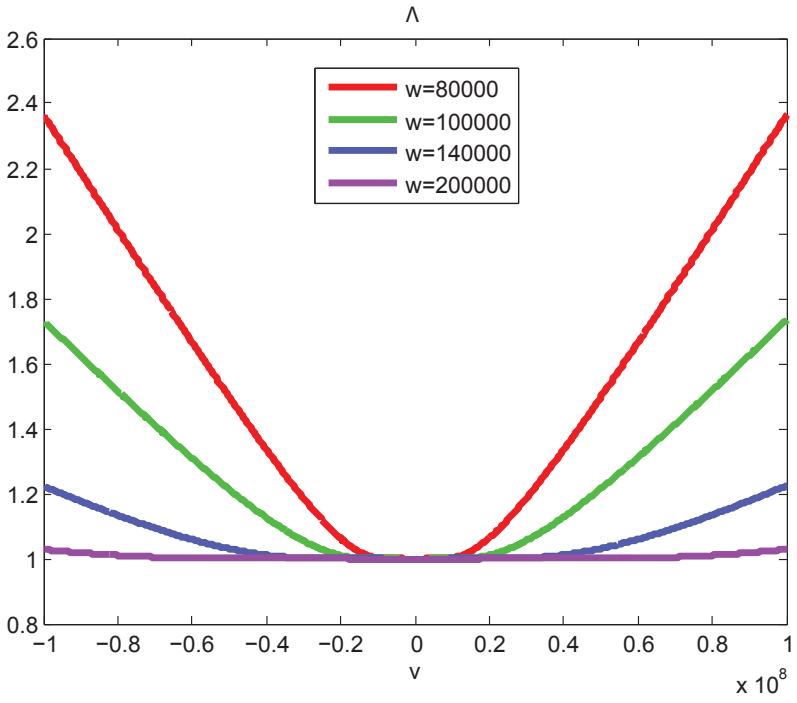

Figure 4. The function $\Lambda(v)$ relating the infinite domain PDF, $\hat{p}(v; w, \psi_0)$, to the truncated domain PDF, $p(v; w, \psi_0)$, for four different precisions of precisions, w. Each curve is essentially made up of an extremely flat portion with $\Lambda = 1$ connected to linearly increasing (decreasing) segments at a rounded corner.

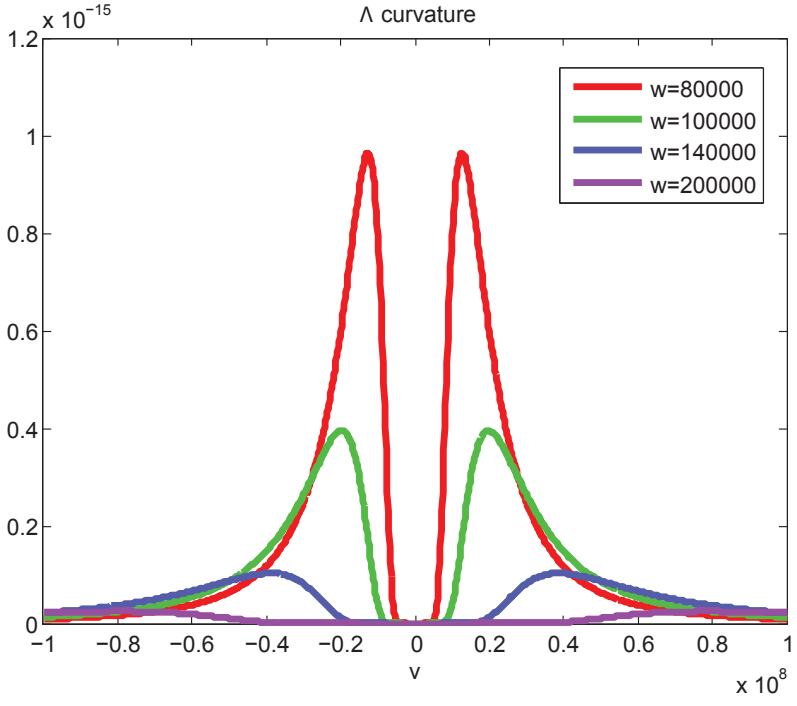

Figure 5. The second derivatives (curvatures) $d^2\Lambda/dv^2$ corresponding to the Λ curves of Figure 4. Notice the extremely small values in a wide range around $v = 0$ and the two narrow peaks where the transition from an almost constant Λ value of one to a straight incline takes place.

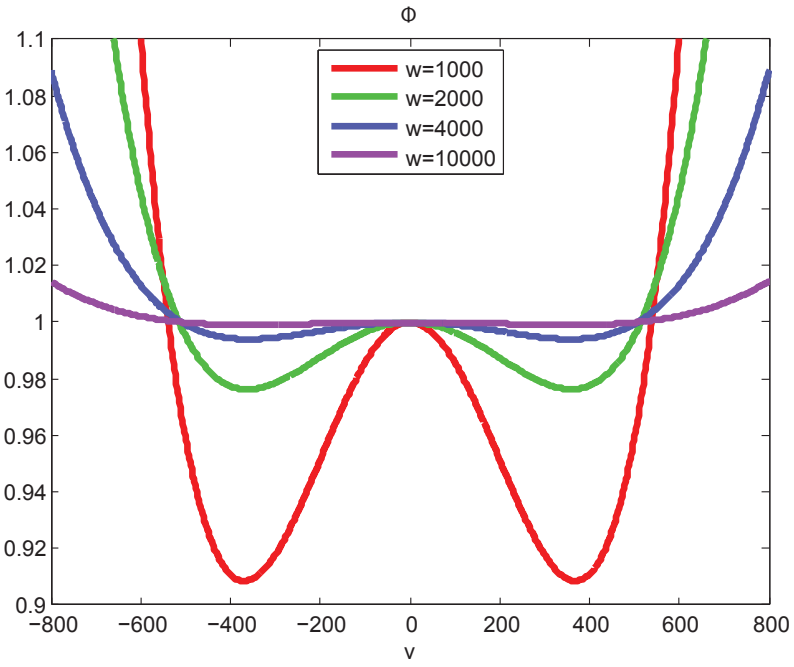

Figure 6. The function $\Phi(v)$ relating the PDF with an exact precision p_{ψ_0} to the PDF $\hat{p}(v; w, \psi_0)$ with a distribution of precisions for four different precisions of precisions w. The two minima disappear over a fairly small w range. Notice that v and w are on different scales from the previous figures in order to show this effect clearly.

Because $p(v; w, \psi_0) = p_{\psi_0}\Phi\Lambda$, investigating Φ also informs us about the scaling function for $p(v; w, \psi_0)$ in terms of p_{ψ_0}.

This function has a different nature than Λ because it emphasizes the polynomial aspects of $\hat{p}(v; w, \psi_0)$ even in the core of the function where it is most Gaussian in nature. Globally the transition for v large compared to w will still exist, but close to the origin, the sharper peak of the polynomial will dominate causing Φ to decline, while in the case of Λ there was a linear (although exceedingly small) increase. But the exponential will take over eventually as the scaling function must grow fast enough to compensate for the exponentially declining tails. That means there will be minima which are determined by the following.

Taking the derivative of the logarithm of Φ and simplifying,

$$\frac{(v^2+w^2)^2}{\Phi}\frac{d\Phi}{dv} = v\left(2\psi_0^2 v^4 + v^2(4\psi_0^2 w^2 - 3) - 3w^2\right). \tag{20}$$

For horizontal tangents, one has $v = 0$ or

$$v^2 = \frac{-(4\psi_0^2 w^2 - 3) \pm \sqrt{(4\psi_0^2 w^2 - 3)^2 + 24\psi_0^2 w^2}}{4\psi_0^2}. \tag{21}$$

When $4\psi_0^2 w^2 > 3$, which is the case for the standard values described, the + sign produces the real results

$$v = \pm\sqrt{\frac{-(4\psi_0^2 w^2 - 3) + \sqrt{(4\psi_0^2 w^2 - 3)^2 + 24\psi_0^2 w^2}}{4\psi_0^2}}, \tag{22}$$

which is, using the standard values, $v = \pm 358$ m/s. (For the parameters used in Figure 6 the value is ± 369 m/s.) These minima and the maximum at $v = 0$ are depicted in the graph of Φ, Figure 6. The minima represent the largest overestimate of $\hat{p}$ by p_{ψ_0} globally. Outside of the interval defined by these minima, p_{ψ_0} increasingly underestimates $\hat{p}$ as Φ grows unbounded. There are no other horizontal tangents than these three, and for $|v| \ll |w|$ the exponential's positive argument grows as v^2, which swamps the polynomial factor.

Λ told us that close to the origin, when both densities were most Gaussian-like, they were most like each other. This confirmed that the heavy tail behavior was a consequence of the temperature fluctuations. Φ tells a slightly different story. While there is sharp divergence in the tails too, the minima clearly tell us that $\hat{p}(v; w, \psi_0)$ is a rather different object than a pure Gaussian. The implication is that the compound distributions cannot be simply Maxwellians evaluated using different parameter values, as was possible with the simple thermalization of wind. Given that is so, local temperature will not have the significance it had in the Laboratory regime.

6 Maximum velocity

The Maxwellian is classically limited. While its mathematical domain is infinite, physically such a mathematical domain has little meaning. There are no massive particles with unbounded energy in a particular ensemble with fixed energy, let alone particles moving beyond the speed of light. The Maxwellian is strictly classical. It does not consider relativistic aspects at all, which require instead something like the Maxwell–Jüttner distribution (e.g., [15]). Moreover, a finite number of particles with finite energy cannot have an unbounded distribution in any case. At some location the domain must be cut to avoid such physical objections. However, the small contribution from physically objectionable parts of the domain are outweighed by the formal convenience of infinite limits. As mentioned, this happens in spectroscopy where negative frequencies are admitted for convenience. For the most part, this presents no difficulties. Exponential tails defeat any polynomial growth. Formal moments are all well defined, leading to elegant formal relationships between integrals.

All of the distributions in this paper have the Maxwellian as their starting point. Therefore all of the physical difficulties mentioned are present, and all of the composite distributions have similar problems. With a given number of particles of given energies, infinite fluctuations in velocity and temperature are not physically meaningful even if convenient. In any case, infinite physical domains are problematic, which was why we considered p in addition to $\hat{p}$.

In every Maxwellian subsystem a maximum velocity is implied, which thus implies an overall maximum for all of the composite distributions. Even leaving relativistic limits and the uncertainty principle aside, no particle can travel faster than a single particle holding all of the system's energy. Although being an entropically exceptionally improbable situation, this is a rigorous upper bound. Beyond that velocity, v_m, there can be no particles at all, and thus in reality the domain is not infinite. This is far above a common upper bound for v, v_c (i.e. $v_\mathrm{c} \ll v_\mathrm{m}$), since giving all energy to just one particle is a singular case. Clearly $k\theta/2 < v_\mathrm{c} < v_\mathrm{m}$ with the lower bound representing the sharing of energy equally. The upper bound will grow with the system size, but for the purpose of establishing finiteness, it is sufficient. For a given energy, E, and number, N, the Maxwellian v_m is easily computed. The v_m for the Maxwellian is a microscopic property unaffected by the convolutions, so should apply to slow time convolutions equally.

Consider an isolated system consisting of N identical particles. Its total energy is in one-dimensional space, as we have been considering here,

$$E = \sum_{i=1}^{N} \frac{1}{2} m v_i^2 = \frac{1}{2} k\theta N. \tag{23}$$

Putting all energy into one of these particles while all the others are at rest,

$$v_\mathrm{m}^2 = \frac{k\theta N}{m}. \tag{24}$$

There are no particles for $v > v_\mathrm{m}$. But what is the error in pretending that there are? Putting v_m into the PDF at that speed, equation (2) becomes

$$p(v_\mathrm{m}) = \left(\frac{m}{2k\theta}\right)^{1/2} \frac{1}{\sqrt{\pi}} \exp\left(-\frac{N}{2}\right). \tag{25}$$

Quite remarkably the exponential's argument is independent of particle mass as well as temperature. There is only the weak temperature dependence in the pre-factor. This will be an extraordinarily small number with N in the exponent. We may expect $p(v_c)$ to be somewhat larger.

The largest velocities that can be encountered in the composite distributions will likely be well represented by some average of v_c. The issue of the finiteness of domain is somewhat hidden in the Gaussian case. But fluctuating temperatures led to heavy tails, bringing this issue out. They are in of themselves not a problem, but in moments they are. The second moment, which we would use for energy, diverges for both p and $\hat{p}$. This is only a problem if the infinite domains are regarded as physical. Clearly if the convenience of infinite integrals compromises the essential physical reality they must take second place. The infinite domain must be trimmed. Exactly how that ought to be done will be considered in future work.

7 Conclusion

This paper has contemplated the perspective of an observer who would regard the laboratory regime as jiggly and microscopic, much as we see the kinetic or nanoscales. We aimed to get beyond pure speculation by focusing on how the Maxwellian distribution might be seen by such an observer. The window of observation for this observer would be bounded by events that are too close in time to distinguish from his point of view (fast time), which would include our regime. We would regard the putative observer as experiencing slow time. Hence the resulting distribution is described as the slow time Maxwellian.

The technique was to form compound distributions by fluctuating the wind, u, and temperature, T. There were several approaches possible in this regard. Which version the putative observer would actually encounter is unknown, and it is unclear how to determine it explicitly. A range of assumptions were tried computationally, making some simple comparisons. As the various cases did not differ much, we adopted assumptions that made the explicit calculations more straightforward and intuitive. In that regard choosing precision to work with was most helpful. Temperature and velocity emerge with a conjugate quality, which occurs explicitly in the case of thermalizing of wind. But it also appears in a more subtle manner in the precision picture because fluctuating precision led to a normal distribution with its own precision (i.e. the precision of the precision). The latter has units of velocity, and this velocity, w, plays a decisive role in the structure and behavior of the resulting compounded densities. It acts like a reference velocity separating regimes. It divides Gaussian-like structure from heavy tail structure.

An unusual hybrid of Gaussians with heavy tails emerges in this paper as a persistent feature. Heavy tails clearly can be expected to be a feature of the slow time regime. This has some consequences. First the notion of local equilibrium ceases to be strictly valid. There is no straightforward temperature, as there is in the Maxwellian case. There could be other qualities that might play such a role in the slow time regime, but they would not be temperature strictly speaking. If w is large enough, the core would still behave Maxwellian, which would permit a limited return to temperature as long as the core of the PDF is of importance. Second, the wings of the distribution need to be considered from a physical standpoint to avoid divergent moment integrals.

There was a question as to what negative ψ meant. We revised the calculation to be normalized for a truncated Gaussian. This led to two distributions, p and $\hat{p}$. The former differed by a new term in (9), as well as a factor that proves to be very close to 1. It is entirely a result of the breaking of symmetry through the truncated distribution. It is an extraordinarily small number compared to the other term except for large enough v, given the standard values in Appendix A. But truncating is a convenient fix and is not necessarily more physical than allowing negative ψ. A sudden jump is known to cause a Cauchy-like distribution in a signal suddenly switched on followed by exponential decay. This suggests that some other distribution without the jump might not lead to the v^{-2} behavior. Therefore we discount this term which dominates p for larger $|v|$.

The slow time observer is left with a rather different behavior for the ideal gas. There are heavy tails and a nearly Gaussian core, becoming more Gaussian with increasing w. But as the tails are heavy, we observe divergent second moments. Does this mean that energy becomes infinite? Not if there are only a finite num-

ber of particles and finite energy in the underlying system to begin with. The composition of PDFs changes nothing in this regard.

One use for such a PDF is in moment equations that are also considered from a slow time perspective [9]. This could lead to a slow time dynamics, which would be the ultimate goal of thinking from this perspective. Clearly the heavy tails and basic closure problems need to be dealt with in future work.

A Standard values

In order to maintain a solid physical intuition we use typical molecular values for our examples. A standard air temperature is $T_0 = 300$ K and the molecular weight of air is 29 g/mol, so $m = 4.84 \times 10^{-26}$ kg. Thus if we take the variation of the wind speed to be $\sigma_u \sim 5$ m/s, we arrive at the combined temperature $\theta = \sigma_u^2 m/k + T = 300.08$ K and the center precision of speed $\psi_0 = \sqrt{2(\sigma_u^2 + kT_0/m)} \sim 2.42 \times 10^{-3}$ $(\text{m/s})^{-1}$. Since $\psi = \sqrt{2k\theta/m}$ and thus $|d\psi| = (\psi_0)^3 (k/m)|dT|$, a representative value for w would be $w \sim 1/|d\psi| \sim 10^5$ m/s for $|dT| \sim 2.5$ K. Error: The two square roots are inverted, numerical values are correct.

References

[1] C. Essex and B. Andresen, The principal equations of state for classical particles, photons, and neutrinos, *J. Non-Equilib. Thermodyn.* **38** (2013), 293–312.

[2] S. Christiansen and P. Sibani, Linear response subordination to intermittent energy release in off-equilibrium aging dynamics, *N. J. Phys.* **10** (2008), 033013.

[3] P. Bak, Self-organized criticality, *Physica A* **163** (1990), 403–409.

[4] S. H. Hansen, D. Egli, L. Hollenstein and C. Salzmann, Dark matter distribution function from non-extensive statistical mechanics, *New Astronomy* **10** (2005), 379–384.

[5] C. Tsallis, Possible generalization of Boltzmann–Gibbs statistics, *J. Stat. Phys.* **52** (1988), 479–487.

[6] C. T. Miller and W. G. Gray, Thermodynamically constrained averaging theory approach for modeling flow and transport phenomena in porous medium systems: 2. Foundation, *Adv. Water Res.* **28** (2005), 181–202.

[7] C. Schulzky, C. Essex, M. Davison, A Franz and K. H. Hoffmann, The similarity group and anomalous diffusion equations, *J. Phys. A* **33** (2011), 5501–5511.

[8] M. W. Oram, N. G. Hatsopoulos, B. J. Richmond and J. P. Donoghue, Excess synchrony in motor cortical neurons provides redundant direction information with that from coarse temporal measures, *J. Neurophysiol.* **86** (2001), 1700–1716.

[9] C. Essex, Does laboratory-scale physics obstruct the development of a theory for climate?, *J. Geophys. Res. Atmos.* **118** (2013), 1218–1225.

[10] C. Essex, Climate theory versus a theory for climate, *Int. J. Bifurcat. Chaos* **21** (2011), 3477–3487.

[11] S. Serdyukov, Generalized temperature and non-classical heat conduction in rigid bodies, *J. Non-Equilib. Thermodyn.* **38** (2013), 81–96.

[12] D. Jou, A. Sellitto and V. A. Cimmelli, Phonon temperature and electron temperature in thermoelectric coupling, *J. Non-Equilib. Thermodyn.* **38** (2014), 335–361.

[13] B. Yilbas and S. B. Mansoor, Phonon transport and equivalent equilibrium temperature, *J. Non-Equilib. Thermodyn.* **38** (2013), 153–174.

[14] W. Muschick, Contact temperature and internal variables, *J. Non-Equilib. Thermodyn.* **39** (2014), 113–121.

[15] G. Chacón-Acosta, L. Dagdug and H. A. Morales-Técotl, Manifestly covariant Jüttner distribution and equipartition theorem, *Phys. Rev. E* **81** (2010), 021126.

Received March 5, 2015; revised May 7, 2015; accepted May 19, 2015.